

Mining higher-order triadic interactions

Marta Niedostatek*,^{1,2} Anthony Baptista*,^{3,1,2} Jun Yamamoto,⁴ Jürgen Kurths,^{5,6}
Ruben Sanchez Garcia,^{2,7} Ben MacArthur,^{2,7,8} and Ginestra Bianconi^{1,2}

¹*School of Mathematical Sciences, Queen Mary University of London, London, E1 4NS, United Kingdom*

²*The Alan Turing Institute, The British Library, London, NW1 2DB, United Kingdom*

³*Cancer Bioinformatics, School of Cancer and Pharmaceutical Sciences,*

Faculty of Life Sciences and Medicine, King's College London, London, WC2R 2LS, UK

⁴*Department of Network and Data Science, Central European University, Vienna 1100, Austria*

⁵*Potsdam Institute for Climate Impact Research, 14473 Potsdam, Germany*

⁶*Institute of Physics, Humboldt University of Berlin, 12489 Berlin, Germany*

⁷*School of Mathematical Sciences, University of Southampton, Southampton SO17 1BJ, United Kingdom*

⁸*Faculty of Medicine, University of Southampton, Southampton SO17 1BJ, United Kingdom*

Complex systems often involve higher-order interactions which require us to go beyond their description in terms of pairwise networks. Triadic interactions are a fundamental type of higher-order interaction that occurs when one node regulates the interaction between two other nodes. Triadic interactions are found in a large variety of biological systems, from neuron-glia interactions to gene-regulation and ecosystems. However, triadic interactions have so far been mostly neglected. In this article, we propose a theoretical model that demonstrates that triadic interactions can modulate the mutual information between the dynamical state of two linked nodes. Leveraging this result, we propose the Triadic Interaction Mining (TRIM) algorithm to mine triadic interactions from node metadata, and we apply this framework to gene expression data, finding new candidates for triadic interactions relevant for Acute Myeloid Leukemia. Our work reveals important aspects of higher-order triadic interactions that are often ignored, yet can transform our understanding of complex systems and be applied to a large variety of systems ranging from biology to the climate.

I. INTRODUCTION

Higher-order networks [1–5] are key to capturing many-body interactions present in complex systems. Inferring higher-order interactions [6–11] from real, pairwise network datasets is recognised as one of the central challenges in the study of higher-order networks [2, 12], with wide applicability across different scientific domains from biology and brain research [13–15] to finance [16, 17]. When from the knowledge of a pairwise network the problem is inferring the many-body interactions, mining higher-order interactions typically involves generative models and Bayesian approaches based on network structural properties [6, 7, 9, 11, 18]. Note, however that when the inference is performed on the basis on the knowledge of the nodes dynamical state [8, 10], inferring higher-order interactions also requires dynamical considerations.

Triadic interactions [19] are a fundamental type of signed higher-order interaction that are gaining increasing attention from the statistical mechanics community [19–24], since they are not reducible to hyperedges or simplices. A triadic interaction occurs when one or more nodes regulate the interaction between two other nodes. The regulator nodes may either enhance or inhibit the interaction between the other two nodes. Triadic interactions are known to be important in various systems, including: ecosystems [25–27] where one species can regulate the interaction between two other species; neuronal

networks [28], where glial cells regulate synaptic transmission between neurons thereby regulating brain information processing; and gene regulation networks [29, 30], where a modulator can promote or inhibit the interaction between a transcription factor and a target gene. There is mounting evidence that triadic interactions can induce (so far largely unexplored) collective phenomena and dynamical states that can reveal important aspects of complex systems [19–24, 31, 32]. An important advance in this line of research is triadic percolation [19–21], a theoretical framework that captures the non-trivial dynamics of the giant component. Moreover, recent results demonstrate that triadic interactions can have significant effects on stochastic dynamics [24] and learning [22, 23]. However, despite the increasing attention that higher-order interactions are receiving, the detection of triadic interactions from network data and node timeseries, is an important scientific challenge that has not been thoroughly explored [29, 33, 34].

In this article, we formulate a dynamical model in which node variables are affected by triadic interactions, and we propose an information theoretic approach, leading to the Triadic Interaction Mining (TRIM) algorithm, for mining triadic interactions. The proposed dynamical model provides evidence of generative mechanisms by which a triadic interaction can induce a significant variability of the mutual information between two nodes at the end-points of an edge. The TRIM algorithm leverages this finding and mines triadic interactions using knowledge of the network structure and the dynamical variables associated to the nodes. The significance of each putative triadic interaction is then assessed using cross-

* These authors contributed equally to this work

validation with two distinct null models.

In this way, the TRIM algorithm can go beyond monotonicity assumptions regarding the functional form of the regulation of the two linked nodes by the third node (which is at the foundation of previously proposed methods [29]) allowing for broader applications. Significant node triples are also associated with an entropic score function S that grows with the spread of the conditional joint distributions functions of the variables at the two end point of the regulated edge. We test the TRIM algorithm on a benchmark dynamical model, demonstrating its efficiency in detecting true triadic interactions. We also use the TRIM model to mine triadic interactions from gene-expression, to identify ‘trigenic’ processes [35]. We demonstrate that the TRIM algorithm is able to detect known interactions as well as propose a set of new candidate interactions that can then be validated experimentally.

II. TRIADIC INTERACTIONS

A triadic interaction occurs when one or more nodes modulate (or regulate) the interaction between two other nodes, either positively or negatively. A *triadic interaction network* is a heterogeneous network composed of a structural network and a regulatory network encoding triadic interactions (Figure 1). The *structural network* $G_S = (V, E_S)$ is formed by a set V of N nodes and a set E_S of L edges. The *regulatory network* $G_R = (V, E_S, E_R)$ is a signed bipartite network with one set of nodes given by V (the nodes of the structural network), and another set of nodes given by E_S (the edges of the structural network) connected by the regulatory interactions E_R of cardinality $|E_R| = \hat{L}$. The signed regulatory network can be encoded as an $L \times N$ matrix K where $K_{\ell i} = 1$ if node i activates the structural edge ℓ , $K_{\ell i} = -1$ if node i inhibits the structural edge ℓ and $K_{\ell i} = 0$ otherwise. If $K_{\ell i} = 1$, then the node i is called a *positive regulator* of the edge ℓ , and if $K_{\ell i} = -1$, then the node i is called a *negative regulator* of the edge ℓ . It is worth noting that node $i \in V$ cannot serve as both a positive and negative regulator for the same edge ℓ at the same time. However, node i can act as a positive regulator for edge ℓ while simultaneously functioning as a negative regulator for a different edge $\ell' \neq \ell$.

III. THE CONTINUOUS TRIADIC INTERACTION MODEL

Here, we formulate a general synthetic dynamical model for a network with triadic interactions between continuous variables. This model acts as a benchmark to validate the TRIM algorithm proposed here. We assume that each node i of the network is associated with a dynamical variable $X_i \in \mathbb{R}$, and that the dynamical

state of the entire network is encoded in the state vector $\mathbf{X} = (X_1, X_2, \dots, X_N)^T$. The topology of the structural network is encoded in the graph Laplacian matrix \mathbf{L} with elements

$$L_{ij} = \begin{cases} -a_{ij}J & \text{if } i \neq j, \\ \sum_j a_{ij}J & \text{if } i = j, \end{cases} \quad (1)$$

where $\mathbf{A} = (a_{ij})$ is the adjacency matrix of the network, and $J > 0$ is a coupling constant. In the absence of triadic interactions, we assume that the dynamics of the network is associated with a Gaussian process implemented as the Langevin equation

$$d\mathbf{X} = -\frac{\delta \mathcal{H}}{\delta \mathbf{X}} + \Gamma \boldsymbol{\eta}(t), \quad (2)$$

with the Hamiltonian

$$\mathcal{H} = \frac{1}{2} \mathbf{X}^\top (\mathbf{L} + \alpha \mathbf{I}) \mathbf{X}, \quad (3)$$

where $\Gamma > 0$, $\alpha > 0$, and $\boldsymbol{\eta}(t)$ indicates uncorrelated Gaussian noise with

$$\langle \eta_i(t) \eta_j(t') \rangle = \delta_{ij} \delta(t - t'), \quad (4)$$

for all t and t' . The resulting Langevin dynamics are given by

$$d\mathbf{X} = -(\mathbf{L} + \alpha \mathbf{I}) \mathbf{X} dt + \Gamma d\boldsymbol{\eta}(t). \quad (5)$$

We remark that the Hamiltonian \mathcal{H} has a minimum for $\mathbf{X} = \mathbf{0}$, and its depth increases as the value of α increases. In a deterministic version of the model ($\Gamma = 0$), the effect of the structural interactions will not be revealed at stationarity. However, the Langevin dynamics with $\Gamma > 0$ encodes the topology on the network. Indeed, at equilibrium the correlation matrix $C_{ij} = \mathbb{E}((X_i - \mathbb{E}(X_i))(X_j - \mathbb{E}(X_j)))$ is given by

$$C_{ij} = \frac{\Gamma^2}{2} [\mathbf{L} + \alpha \mathbf{I}]_{ij}^{-1}. \quad (6)$$

In other words, from the correlation matrix it is possible to infer the Laplacian, and hence the connectivity of the network.

We now introduce triadic interactions in the model. As explained earlier, a triadic interaction occurs when one or more nodes modulate the interaction between another two nodes. To incorporate triadic interactions into the network dynamics, we modify the definition of the Laplacian operator present in the Langevin equation. Namely, we consider the Langevin dynamics

$$d\mathbf{X} = -(\mathbf{L}^{(T)} + \alpha \mathbf{I}) \mathbf{X} dt + \Gamma d\boldsymbol{\eta}(t), \quad (7)$$

obtained from Eq.(2) by substituting the graph Laplacian \mathbf{L} with the *triadic Laplacian* $\mathbf{L}^{(T)}$ whose elements are given by

$$L_{ij}^{(T)} = \begin{cases} -a_{ij}J_{ij}(\mathbf{X}) & \text{if } i \neq j, \\ \sum_{k=1}^N a_{ik}J_{ik}(\mathbf{X}) & \text{if } i = j. \end{cases} \quad (8)$$

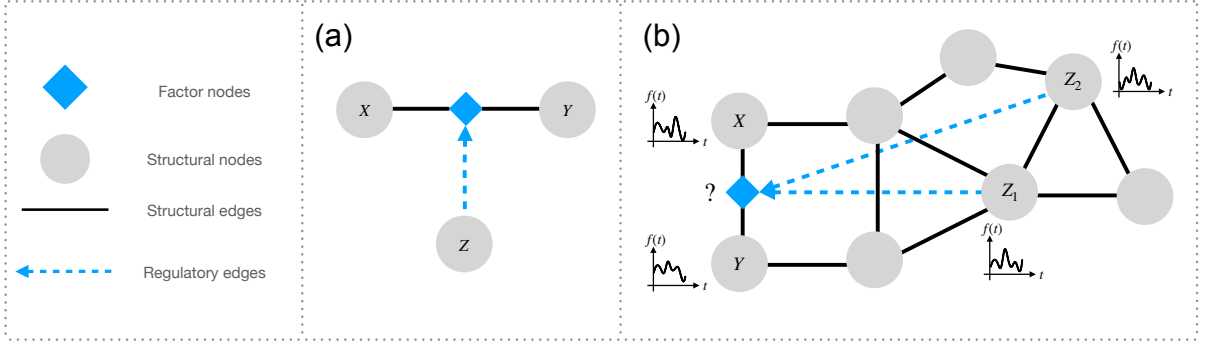


Figure 1. (Panel a) A triadic interaction occurs when a node Z , called a *regulator node*, regulates (either positively or negatively) the interaction between two other nodes X and Y . The regulated edge can be conceptualised as a *factor node* (shown here as a cyan diamond). (Panel b) A network with triadic interactions can be seen as a network of networks formed by a simple structural network and by a bipartite regulatory network between regulator nodes and regulated edges (factor nodes).

Moreover, we assume that the coupling constants $J_{ij}(\mathbf{X})$ are determined by a perceptron-like model that considers all the regulatory nodes of the link $\ell = [i, j]$ and the sign of the regulatory interactions. Specifically, if $\sum_{k=1}^N K_{\ell k} X_k \geq \hat{T}$ then we set $J_{ij} = w_+$; if instead $\sum_{k=1}^N K_{\ell k} X_k < \hat{T}$ then we set $J_{ij} = w_-$, with $w_+, w_- \in \mathbb{R}_+$ and $w_+ > w_-$. Thus, we set

$$J_{ij}(\mathbf{X}) = w_- + (w_+ - w_-) \theta \left(\sum_{k=1}^N K_{\ell k} X_k - \hat{T} \right), \quad (9)$$

where $\theta(\cdot)$ is the Heaviside function ($\theta(x) = 1$ if $x \geq 0$ and $\theta(x) = 0$ if $x < 0$). Note that, in the presence of triadic interactions, the stochastic differential equation (7) is not associated with any Hamiltonian, and a stationary state of the dynamics is not guaranteed, making this dynamical process significantly more complex than the original Langevin dynamics given in Eq.(2). This generic model of triadic interactions is related to a recently proposed model that captures information propagation in multilayer networks [24], but does not make use of a multilayer representation of the data. Moreover the model is significantly different from models of higher-order interactions previously proposed in the context of consensus dynamics [36, 37] or contagion dynamics [38, 39]. Indeed, in our framework, triadic interactions between continuous variables are not reducible to standard higher-order interactions because they involve the modulation of the interaction between pair of nodes. Moreover, this modulation of the interaction is not dependent on the properties of the interacting nodes and their immediate neighbours such as in [36, 37] or in the machine learning attention mechanism [40]. On the contrary, the modulation of the interaction is determined by a third regulatory node (or a larger set of regulatory nodes) encoded in the regulatory network.

Our model of triadic interactions, therefore, has the crucial property that triadic interactions are higher-order interactions that cannot be reduced to pairs of pairwise interactions. An important problem that then arises is

whether such interactions can be mined from observational data. To address this issue, we will develop a new algorithm – that we call the TRIM algorithm – to identify triadic interactions from data, and we will test its performance on the data generated from the model described above.

IV. MINING TRIADIC INTERACTIONS

A. The TRIM algorithm

We propose the TRIM algorithm (see Figure 2) to mine triadic interactions among triples of nodes. To simplify the notation we will use the letters X, Y, Z to indicate both nodes as well as their corresponding dynamical variables.

Given a structural edge between nodes X and Y , our goal is to determine a confidence level for the existence of a triadic interaction involving an edge between node X and node Y with respect to a potential regulator node Z . Specifically, we aim to determine whether the node Z regulates the edge between node X and node Y , given the dynamical variables X, Y and Z associated with these nodes. To do so, given a time series associated with node Z , we first sort the Z -values, and define P bins in terms of the quantiles of z , chosen in such a way that each bin m_z comprises the same number of data points (ranging in our analyses from 30 to 100). We indicate with z_m the quantile of Z corresponding to the percentile m/P . Therefore, each bin m_z indicates data in which Z ranges in the interval $[z_m, z_{m+1})$. We indicate with $\mu(x|z_m), \mu(y|z_m)$ and $\mu(x, y|z_m)$ the probability density of the variables X, Y and the joint probability density of the variables X and Y in each m_z bin.

A triadic interaction is taken to occur when the node Z affects the strength of the interaction between the other two nodes X and Y . Consequently, our starting point is to consider the mutual information between the dynamical variables X and Y conditional to the specific value of

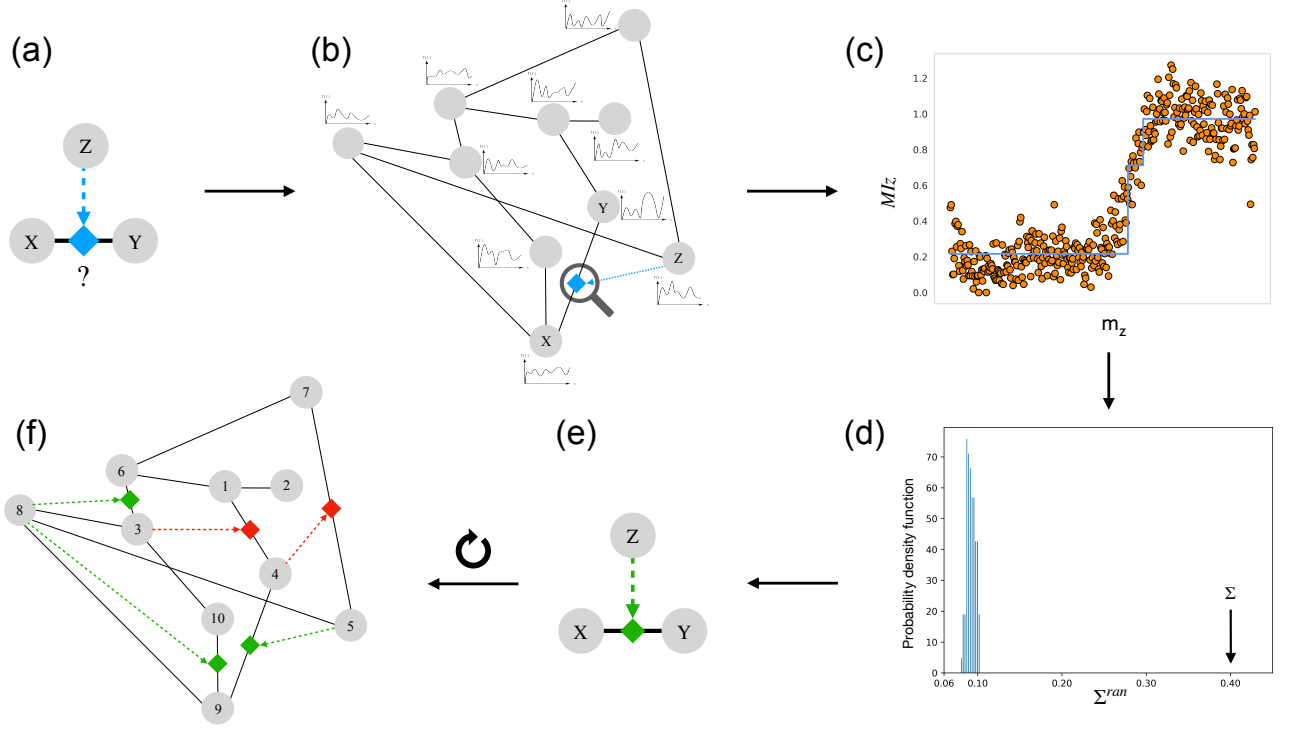


Figure 2. The TRIM algorithm identifies triples of nodes X , Y , and Z involved in a putative triadic interaction, starting from the knowledge of the structural network and the dynamical variables associated with its nodes. For each putative triple of nodes involved in a triadic interaction (panel (a)) which belong to a network whose structure and dynamics is known (panel (b)), we study the functional behavior of the conditional mutual information MIz (panel (c)), and assess the significance of the observed modulations of MIz with respect to a null model (panel (d)). Given a predetermined confidence level, we can use these statistics to identify significant triadic interactions (panel (e)). This procedure can be extended to different triples of the network, thereby identifying the triadic interactions present in it (panel (f)).

the dynamical variable Z . We thus consider the quantity $MIz(m) = MI(X, Y|Z = z_m)$ defined as

$$MIz(m) = \int dx \int dy \mu(x, y|z_m) \log \left(\frac{\mu(x, y|z_m)}{\mu(x|z_m)\mu(y|z_m)} \right).$$

In order to estimate this quantity, we rely on non-parametric methods based on entropy estimation from k -nearest neighbors [41–43]. For each triple of nodes, we visualize the mutual information MIz computed as a function of the m/P -th quantiles z_m and fit this function with a decision tree comprising r splits.

In the absence of triadic interactions, we expect MIz to be approximately constant as a function of the m/P -th quantiles z_m , while, in the presence of triadic interactions, we expect this quantity to vary significantly as a function of z_m . The discretized conditional mutual information CMI between X and Y conditioned on Z can be written as

$$CMI_{X,Y;Z} = \sum_{m=0}^{P-1} p(z_m) MIz(m) = \langle MIz \rangle, \quad (10)$$

where $p(z_m) = 1/P$ indicates the probability that the Z value falls in the m_z bin. This quantity indicates impor-

tant information about the interaction between the nodes X and Y when combined with the information coming from the mutual information MI given by

$$MI_{X,Y} = \int dx \int dy \mu(x, y) \log \left(\frac{\mu(x, y)}{\mu(x)\mu(y)} \right),$$

where $\mu(x)$, $\mu(y)$ are the probability density functions for X and Y and $\mu(x, y)$ is the joint probability density functions of the variables X and Y . In particular, true interactions between X and Y are typically associated with both high mutual information MI and high conditional mutual information CMI .

The conditional mutual information CMI , however, is not sensitive to variations in MIz and does not therefore provide the information needed to detect triadic interactions. In order to overcome this limitation, we define the following three quantities that measure how much the mutual information between X and Y conditioned on $Z \in [z_m, z_{m+1})$ changes as z_m varies. Specifically we consider:

- (1) the standard deviation Σ of MIz , defined as

$$\Sigma = \sqrt{\sum_{m=0}^{P-1} p(z_m) [MIz(m) - \langle MIz \rangle]^2}; \quad (11)$$

- (2) the difference T between the maximum and minimum value of MIz , given by

$$T = \max_{m=0, \dots, P-1} |MIz(m) - \langle MIz \rangle|. \quad (12)$$

The quantities Σ , T , collectively measure the strength of the triadic interaction under question and can thus be used to mine triadic interactions in synthetic as well as in real data. In order to assess the significance of the putative triadic interaction, we compare the observed values of these variables to the results obtained with given null models. In order to determine if the observed values are significant with respect to a given null model, we compute the scores Θ_Σ , Θ_T , given by

$$\begin{aligned} \Theta_\Sigma &= \frac{\Sigma - \mathbb{E}(\Sigma^{\text{ran}})}{\sqrt{\mathbb{E}((\Sigma^{\text{ran}})^2) - (\mathbb{E}(\Sigma^{\text{ran}}))^2}}, \\ \Theta_T &= \frac{T - \mathbb{E}(T^{\text{ran}})}{\sqrt{\mathbb{E}((T^{\text{ran}})^2) - (\mathbb{E}(T^{\text{ran}}))^2}}, \end{aligned} \quad (13)$$

and the p -values

$$p_\Sigma = \mathbb{P}(\Sigma^{\text{ran}} > \Sigma), \quad p_T = \mathbb{P}(T^{\text{ran}} > T), \quad (14)$$

Note that if we consider \mathcal{N} realizations of the null model, we cannot estimate probabilities smaller than $1/\mathcal{N}$. Therefore, if in our null model we observe no value of Σ^{ran} larger than the true data Σ , we set the conservative estimate $p_\Sigma = 1/\mathcal{P}$. A similar procedure is applied also to p_T .

In this work we have considered two types of null models. The first is the randomization null model obtained by shuffling the Z values, to give \mathcal{N} randomization of the data, i.e. we use surrogate data for testing [44, 45]. The second is the maximum likelihood Gaussian null model between the three nodes involved in the triple X, Y, Z . We note that the adoption of these two null models allows us to also potentially capture non-monotonic relationships between MIz and z , thereby going beyond underlying monotonic assumptions made in [46]. The first null model disrupts the temporal correlations between the timeseries of the node Z and the timeseries the two nodes X and Y at the endpoints of the considered edges. Therefore this null model is robust with respect to the presence of possible outliers in the dataset. However this first null model may overlook confounding network effects that affect correlations between the dynamical variables. The second null model more efficiently captures correlations between the dynamical state of the three considered nodes due to network effects but is more sensitive to the

presence of outliers in the data. To increase confidence, we therefore combine the insights coming from both null models (see SI for details).

For each triple, the function $MIz(m)$ is fitted with a decision tree with two splits. In this way, three different intervals of values of Z are identified, each corresponding to a distinct functional behavior of the correlation functions between the variables X and Y . While the method would allow for more than two splits of the decision tree in general, here we have chosen three splits as this is the minimum number of splits that will allow us to capture non-trivial functional behaviour of MIz , like non-monotonicity. In practice this will be the best choice in presence of limited data and a small number of bins as in the Gene Expression data we will analyse in the following.

We further characterize significant triples by examining their entropic score function S , which is used to characterize their corresponding functional behaviour, as described in the SI.

As we will discuss below, the algorithm performs well on our paradigmatic model. Moreover, while the results obtained with the randomized surrogate data might neglect potentially important network effects, this shortcoming of this approach is mitigated by the cross-validation with the Gaussian null model.

B. Validation of the TRIM algorithm on the triadic interaction model

To demonstrate the efficacy of the TRIM algorithm we first considered a single network (see Figure 4(a)) of $N = 10$ nodes, $L = 12$ edges and $\hat{L} = 5$ triadic interactions (each formed by a single node regulating a single edge) on top of which we consider the triadic dynamical model proposed in Sec. III.

Simulations of Eq. (7) on this network show a strong dependence of $MIz(m)$ on m for the triples of nodes involved in triadic interactions, with greater significance for smaller values of α . Figure 3 shows the joint distributions $P_\alpha(X, Y)$ of X and Y for each interval α of values Z determined by the decision tree. The results provide evidence of this interesting dynamical behavior of the triadic model in the case of a positive regulatory interaction. Note that our analysis of the function $MIz(m)$ also allows us to distinguish between positive and negative regulatory interactions. These are associated respectively by an increase in MIz for larger values of z_m or decrease of MIz . In the Supplementary Figures S1-S2, we display further examples of the function MIz for triadic triples. We observe that as the parameter Γ is raised, i.e. the noise increases, which is reflected in the increased variability of the MIz functional behavior.

In order to provide an overall assessment of the performance of TRIM in mining triadic interactions on this network, in Figure 4(b) we display the Receiver Operating Characteristic curve (ROC curve) based on the score

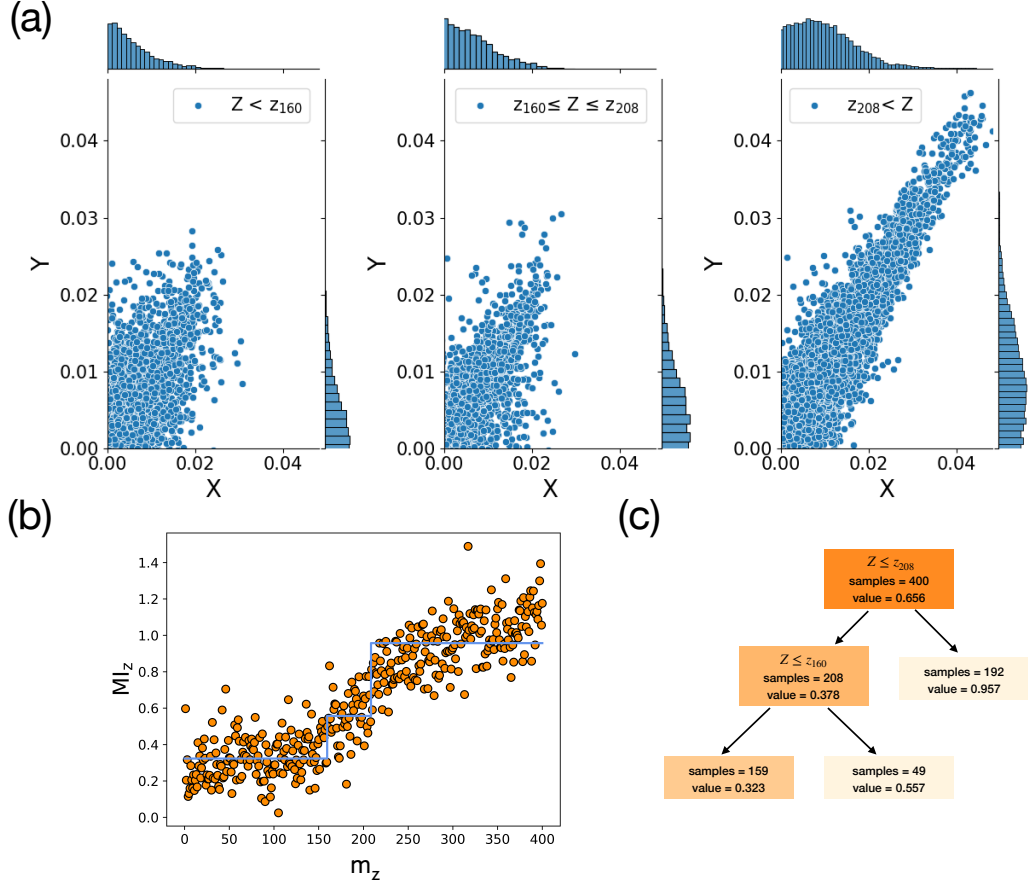


Figure 3. Representative results for triples of nodes involved in triadic interactions in the continuous model with triadic interactions. The joint distributions of variables X and Y conditional on the values of Z are shown in panel (a). Panel (b) shows the behavior of MIz as a function of the values of z_m , which clearly departs from the constant behavior expected in absence of triadic interactions. Panel (c) presents the decision tree for fitting the MIz functional behavior and determining the range of values of Z for which the most significant differences among the joint distributions of the variables X and Y conditioned on Z are observed. For more details about the simulation results, see the Supplementary Information (SI).

Θ_Σ , measured with respect to the first null model which we found to perform well for a wide range of parameters. As it is apparent from the ROC curve, the TRIM algorithm performs better for higher values of α and smaller values of Γ (see Figure 4(b)). For any values of the parameters, we notice that the false positives are more likely to involve short-range triples, i.e. triples in which the regulator node Z has short (small) structural network distance with the two nodes X and Y .

We conclude our discussion by testing the TRIM algorithm on a much larger model network, to demonstrate its scalability. To this end, we consider a random network of 100 nodes, 110 edges, and 25 triadic interactions (see SI for details). In Figure 5 we report the results of the TRIM algorithm for all the triples involving all edges, 14 of which come from the pool of edges with triadic interactions. For each edge, all possible triples are analysed while for each edges we retain only the 5 most significant triples according to Θ_Σ . By conditioning on the value of third node, for each of these connected nodes we also

record the conditional mutual information CMI. In figure 5, each considered triple corresponds to a point, colour coded according to the value of S . Stars indicate triples that are involved in a triadic interactions (see SI for details). The true triadic interactions are indeed found for triples with high Θ_Σ score, while CMI and S span between high and intermediate values.

V. DETECTING TRIADIC INTERACTIONS IN GENE-EXPRESSION DATA

Searching for trigenic interactions in gene-expression is a problem of major interest in biology. For instance, understanding the extent to which a modulator promotes or inhibits the interplay between a transcription factor and its target gene is crucial for deciphering gene regulation mechanisms. In order to address this question with our method, we considered gene-expression data from Acute Myeloid Leukemia (AML), extracted from

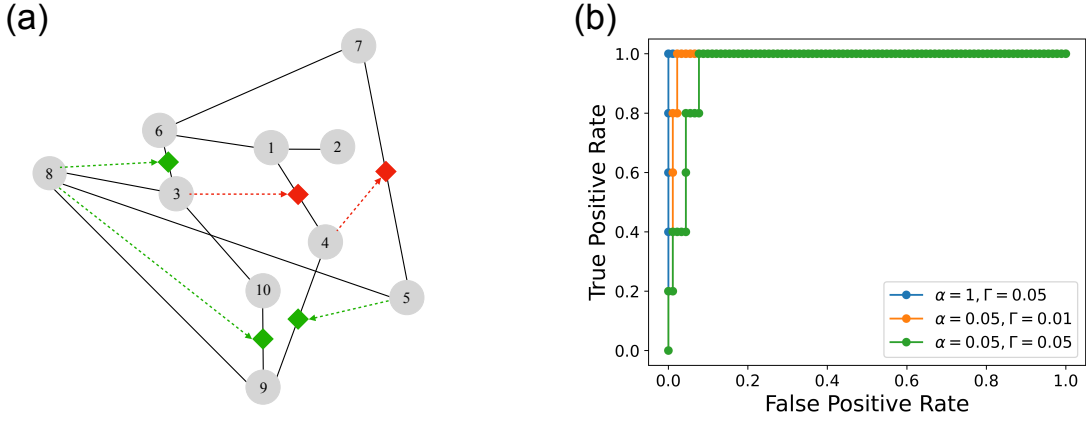


Figure 4. We consider a network with $N = 10$, nodes $L = 12$ edges, and $\hat{L} = 5$ regulatory interactions (panel (a)). The time series obtained by integrating the stochastic dynamics of the proposed dynamical model for triadic interactions (Eq.(7)) are analyzed with the TRIM algorithm. Panel (b) displays the Receiver Operating Characteristic curve (ROC curve) obtained by running TRIM with $P = 400$ bins and $\mathcal{N} = 10^3$ realizations of the null model on these synthetic time series, using Θ_Σ to score for different parameters values indicated in the legend. The time series is simulated up to a maximum time $t_{max} = 4000$ with a $dt = 10^{-2}$. For the analysis, we consider 40000 time steps (see the SI for details). The parameters of the model are: $\hat{T} = 10^{-3}$, $w^+ = 8$, $w^- = 0.5$, and α and Γ as indicated in the figure legend.

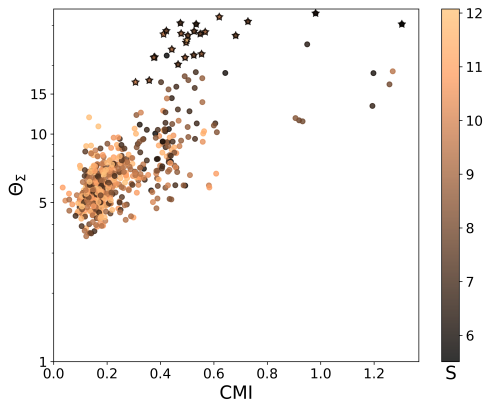


Figure 5. Performance of the TRIM algorithm on a benchmark network with triadic interactions. Each data point shows measures for a triple of nodes X , Y and Z , namely Θ_Σ and CMI, the proposed Σ -score and conditional mutual information between X and Y , respectively. The colour of each point corresponds to the value of S , which characterises the entropy of the triple. The synthetic data comes from a network with 100 nodes, 110 edges, and 25 triadic interactions. All possible triples are represented in the scatter plot. Stars are the true triadic triples.

the Grand Gene Regulatory Network Database [50, 51].

Exhaustive mining of all potential triadic interactions among each triple of nodes in the AML dataset is computationally very demanding (it would require testing of $> 260M$ triplets). Instead, we here focus on edges associated with known biophysical interactions, as identified in the human Protein-Protein Interaction network (PPI)

[50]. To do so, we considered the subgraph of the human PPI network that contains all the genes/proteins included in the AML gene expression data. The number of edges in this subgraph is $M = 42,511$. We first selected a set of triples involving genes known to be associated to AML with gene X and Y connected by an edge in the PPI (see SI for details). Moreover we selected additional triples according to a criteria based on the positions of the three genes in the Maximum Spanning Tree (MST) which only includes 621 edges (see Figure 6). For each edge in the MST, connecting gene X with gene Y we consider all genes Z within a distance of 4 from both the X and Y as candidate regulatory nodes, i.e. the third node in the triple (see SI for details). For each considered triple of genes we use Θ_Σ as the significance score, with $P = 5$ bins, using $\mathcal{N} = 5 \times 10^3$ realizations of the randomization null model. These results have strong correlations with the results obtained considering Θ_T as the significance score (see Supplementary Figures S3-S4 for comparison).

Figure 7 shows the result of the TRIM algorithm for a selected set of the analysed triples with $p_\Sigma < 0.001$. Specifically, the figure displays each triple in the plane Θ_Σ and CMI with a colour code encoding the value S . Note that for each selected edge only the top 5 triples ranked according to the Θ_Σ score are depicted. Squares indicate triples chosen from biologically relevant genes for AML. Crosses indicate triples deemed insignificant in comparison with the Gaussian null model, Figures 7B and 7C provide examples of conditional distributions of two exemplary triples with high entropic score S . Both triples show evidence of triadic interactions: the triple in panel B is a member of the MST, while C is an example of a triple chosen from known biologically relevant

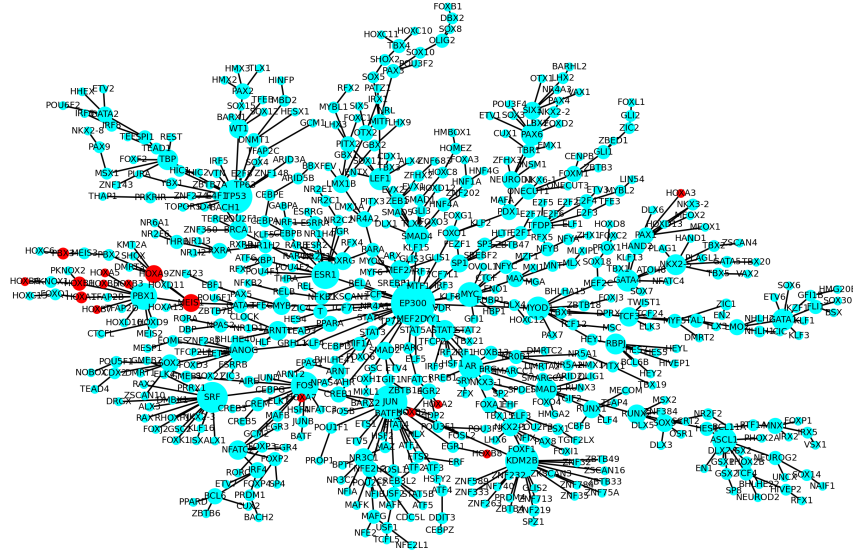


Figure 6. Maximal Spanning Tree of the relevant genes from the gene expression data. Edges and their edge weights are obtained from the Protein-Protein interaction network. Red-coloured nodes are nodes with biological significance, that is that play a critical role in AML[47][48][49]. Node size is proportional to the node degree.

genes for AML. For further examples of results obtained on more gene-expression triples, see the SI for details. Interestingly, among the significant triples, we detected also triples in which the modulation of the mutual information is non-monotonic (see SI for details).

Many of the genes involved in the 50 highest ranking triples have already been linked to AML in the literature (see SI for Table 2 for a list of highly significant triples and Figure S6 with links to the literature associating the involved genes with AML). Interestingly, genes such as PAX4, SOX14 and VAX2 which appear in multiple triples have been found to be over- or under-expressed in patients with AML. Remarkably, 2 such genes, ASCL1 and NEUROG2, are involved in 5 triples, suggesting that they may play a particularly important part in disease progression [52]. In total, 61% of genes in the triples have a known association with AML.

VI. CONCLUSIONS

This work provides a comprehensive information theory-based framework to model and mine triadic interactions directly from dynamic observations and for previous knowledge of the underlying pairwise network. The generative model we propose demonstrates that the presence of a triadic interaction leads to the modulation of the mutual information between the two end nodes of an edge (X and Y) by a third regulatory node Z. Via this model we show that to detect triadic interactions it is necessary to go beyond standard pairwise measures, such as

the mutual information. Moreover, also standard higher-order statistical measures such as the conditional mutual information that only account for the average effect of the third regulatory node Z on the mutual information between X and Y falls short in characterizing triadic interactions. Our proposed approach, implemented in the TRIM algorithm, mines triadic interactions based on the quantification of the statistically significant modulation of the mutual information between the two linked nodes conditioned on the third regulator node. This algorithm is tested and validated on our generative model using paradigmatic random networks with triadic interactions and used to mine putative triadic interactions from gene expression data.

From the network theory point of view, this work opens new perspectives in the active field of modelling and inference of higher-order interactions and can be extended in many different directions, for instance by exploring the effect of triadic interactions on the dynamical state of nodes associated with discrete variables. From the biological point of view, our results may inspire further information-theoretic approaches to genetic regulatory network inference. Investigating the extent to which triadic interactions are tissue-specific, and if certain regulatory patterns are conserved across different tissues, could yield valuable insights. Our proposed approach could also be used to mine triadic interactions in other domains, such as finance or climate, where triadic interactions also have a significant role.

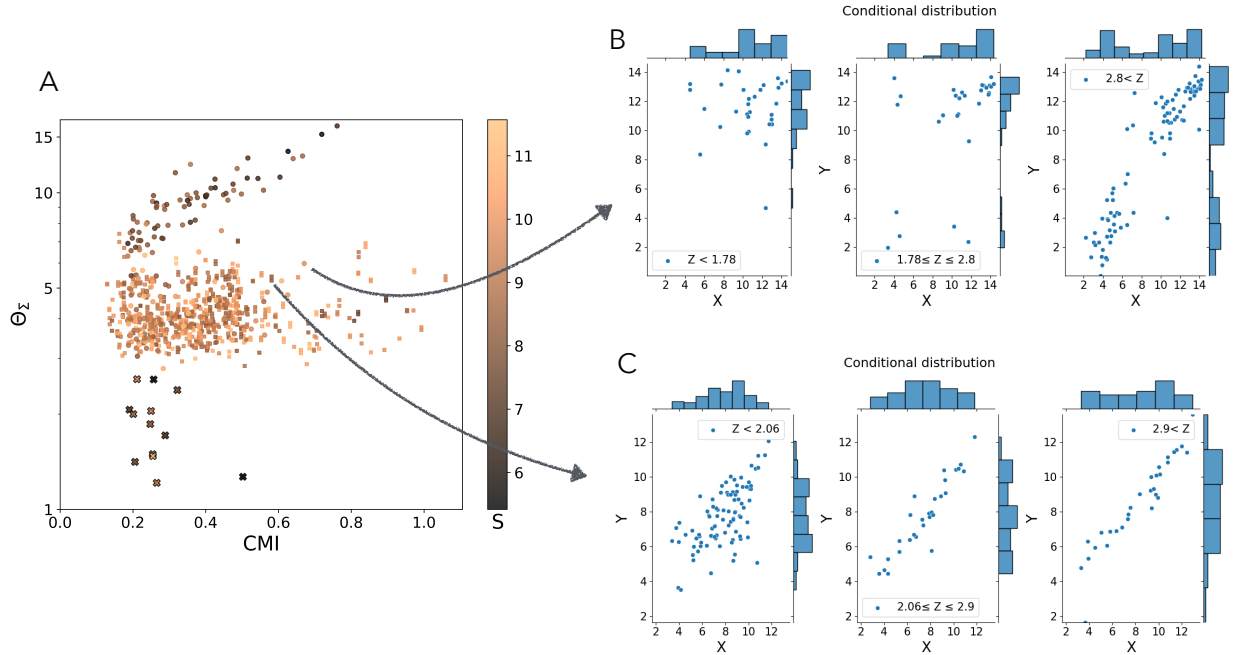


Figure 7. (A) Scatter plot which displays Θ_Σ (Y-axis) and the CMI (X-axis) value between two genes, denoted X and Y , conditioned by a third gene, denoted Z . The colour corresponds to the value of our entropy measure S . Here only triples are depicted that rank among the 300 highest for CMI and MI and have p -value 0.001 or less in the randomization null model. Circles are triples resulting from the MST, whereas squares are triples involving genes with biological relevance. Crosses are triples that have p -value bigger than 0.0005 with the Gaussian version null model. (B) The results of the decision tree allow us to distinguish three intervals in the value of Z in which the conditional distribution of the gene expression of X and Y differs the most. Plots of these conditional distributions are provided for two exemplary triples: both display a high significance score for the triadic interaction, indicating a meaningful biological association. The top row shows three biologically relevant genes, ($X = \text{HOXB3}$, $Y = \text{MEIS1}$, $Z = \text{GLIS3}$, $\Theta_\Sigma = 5.2$, $p_\Sigma = 0.0001$, $\Sigma = 0.38$); the bottom row shows a triples identified by the MST. (C) has p_Σ -value 0.0001 in the random version. ($X = \text{GATA1}$, $Y = \text{KLF1}$, $Z = \text{ETV1}$, $\Theta_\Sigma = 6.1$, $\Sigma = 0.44$)

CODE AVAILABILITY

The Python package triaction is available on GitHub at the following link: <https://github.com/anthbapt/triaction>

<https://doi.org/10.5281/zenodo.438045>. M.N. A.B., R. S.-G. and G. B. acknowledge support from the Turing-Roche North Star partnership.

ACKNOWLEDGMENTS

This research utilized Queen Mary's Apocrita HPC facility, supported by QMUL Research-IT,

-
- [1] Ginestra Bianconi. *Higher-Order Networks*. Elements in the Structure and Dynamics of Complex Networks. Cambridge University Press, Cambridge, 2021.
 - [2] Federico Battiston, Enrico Amico, Alain Barrat, Ginestra Bianconi, Guilherme Ferraz de Arruda, Benedetta Franceschiello, Iacopo Iacopini, Sonia Kéfi, Vito Latora,

- Yamir Moreno, Micah M. Murray, Tiago P. Peixoto, Francesco Vaccarino, and Giovanni Petri. The physics of higher-order interactions in complex systems. *Nature Physics*, 17(10):1093–1098, 2021.
- [3] Federico Battiston, Giulia Cencetti, Iacopo Iacopini, Vito Latora, Maxime Lucas, Alice Patania, Jean-Gabriel

- Young, and Giovanni Petri. Networks beyond pairwise interactions: structure and dynamics. *Physics Reports*, 874:1–92, 2020.
- [4] Leo Torres, Ann S Blevins, Danielle Bassett, and Tina Eliassi-Rad. The why, how, and when of representations for complex systems. *SIAM Review*, 63(3):435–485, 2021.
 - [5] Christian Bick, Elizabeth Gross, Heather A. Harrington, and Michael T. Schaub. What are higher-order networks?, 2022.
 - [6] Jean-Gabriel Young, Giovanni Petri, and Tiago P. Peixoto. Hypergraph reconstruction from network data. *Communications Physics*, 4(1):135, 2021.
 - [7] Martina Contisciani, Federico Battiston, and Caterina De Bacco. Inference of hyperedges and overlapping communities in hypergraphs. *Nature Communications*, 13(1):7229, 2022.
 - [8] Federico Malizia, Alessandra Corso, Lucia Valentina Gambuzza, Giovanni Russo, Vito Latora, and Matia Frasca. Reconstructing higher-order interactions in coupled dynamical systems. *Nature Communications*, 15(1):5184, 2024.
 - [9] Federico Musciotto, Federico Battiston, and Rosario N Mantegna. Detecting informative higher-order interactions in statistically validated hypergraphs. *Communications Physics*, 4(1):218, 2021.
 - [10] Robin Delabays, Giulia De Pasquale, Florian Dörfler, and Yuanzhao Zhang. Hypergraph reconstruction from dynamics. *arXiv preprint arXiv:2402.00078*, 2024.
 - [11] Simon Lizotte, Jean-Gabriel Young, and Antoine Allard. Hypergraph reconstruction from uncertain pairwise observations. *Scientific Reports*, 13(1):21364, 2023.
 - [12] Fernando E Rosas, Pedro AM Mediano, Andrea I Luppi, Thomas F Varley, Joseph T Lizier, Sebastiano Stramaglia, Henrik J Jensen, and Daniele Marinazzo. Disentangling high-order mechanisms and high-order behaviours in complex systems. *Nature Physics*, 18(5):476–477, 2022.
 - [13] Fernando E Rosas, Pedro AM Mediano, Michael Gastpar, and Henrik J Jensen. Quantifying high-order interdependencies via multivariate extensions of the mutual information. *Physical Review E*, 100(3):032305, 2019.
 - [14] Sebastiano Stramaglia, Tomas Scagliarini, Bryan C Daniels, and Daniele Marinazzo. Quantifying dynamical high-order interdependencies from the o-information: An application to neural spiking dynamics. *Frontiers in Physiology*, 11:595736, 2021.
 - [15] Eckehard Olbrich, Nils Bertschinger, and Johannes Rauh. Information decomposition and synergy. *Entropy*, 17(5):3501–3517, 2015.
 - [16] Guido Previde Massara, Tiziana Di Matteo, and Tomaso Aste. Network filtering for big data: Triangulated maximally filtered graph. *Journal of complex Networks*, 5(2):161–178, 2016.
 - [17] Michele Tumminello, Tomaso Aste, Tiziana Di Matteo, and Rosario N Mantegna. A tool for filtering information in complex systems. *Proceedings of the National Academy of Sciences*, 102(30):10421–10426, 2005.
 - [18] Anatol E Wegner and Sofia C Olhede. Nonparametric inference of higher order interaction patterns in networks. *Communications Physics*, 7(1):258, 2024.
 - [19] Hanlin Sun, Filippo Radicchi, Jürgen Kurths, and Ginestra Bianconi. The dynamic nature of percolation on networks with triadic interactions. *Nature Communications*, 14(1):1308, 2023.
 - [20] Ana P Millán, Hanlin Sun, Joaquín J Torres, and Ginestra Bianconi. Triadic percolation induces dynamical topological patterns in higher-order networks. *arXiv preprint arXiv:2311.14877*, 2023.
 - [21] Hanlin Sun and Ginestra Bianconi. Higher-order triadic percolation on random hypergraphs. *Physical Review E*, 110(6):064315, 2024.
 - [22] Lukas Herron, Pablo Sartori, and BingKan Xue. Robust retrieval of dynamic sequences through interaction modulation. *PRX Life*, 1(2):023012, 2023.
 - [23] Leo Kozachkov, Jean-Jacques Slotine, and Dmitry Krotov. Neuron-astrocyte associative memory. *arXiv preprint arXiv:2311.08135*, 2023.
 - [24] Giorgio Nicoletti and Daniel Maria Busiello. Information propagation in multilayer systems with higher-order interactions across timescales. *Physical Review X*, 14(2):021007, 2024.
 - [25] Eyal Bairey, Eric D. Kelsic, and Roy Kishony. High-order species interactions shape ecosystem diversity. *Nature Communications*, 7(1):12285, 2016.
 - [26] Jacopo Grilli, György Barabás, Matthew J. Michalska-Smith, and Stefano Allesina. Higher-order interactions stabilize dynamics in competitive network models. *Nature*, 548(7666):210–213, 2017.
 - [27] Andrew D. Letten and Daniel B. Stouffer. The mechanistic basis for higher-order interactions and non-additivity in competitive communities. *Ecol Lett*, 22(3):423–436, March 2019.
 - [28] Woo-Hyun Cho, Ellane Barcelon, and Sung Joong Lee. Optogenetic glia manipulation: Possibilities and future prospects. *Experimental Neurobiology*, 25(5):197–204, October 2016.
 - [29] Kai Wang, Masumichi Saito, Brygida C. Bisikirska, Mariano J. Alvarez, Wei Keat Lim, Presha Rajbhandari, Qiong Shen, Ilya Nemenman, Katia Basso, Adam A. Margolin, Ulf Klein, Riccardo Dalla-Favera, and Andrea Califano. Genome-wide identification of post-translational modulators of transcription factor activity in human b cells. *Nature Biotechnology*, 27(9):829–837, 2009.
 - [30] Federico M. Giorgi, Gonzalo Lopez, Jung H. Woo, Brygida Bisikirska, Andrea Califano, and Mukesh Bansal. Inferring protein modulation from gene expression data using conditional mutual information. *PLOS ONE*, 9(10):e109569, October 2014.
 - [31] Jie Gao, Jianfeng Luo, Xing Li, Yihong Li, Zunguang Guo, and Xiaofeng Luo. Triadic percolation in computer virus spreading dynamics. *Chinese Physics B*, 34(2):028701, 2025.
 - [32] Mateusz Iskrzyński, Aleksandra Puchalska, Aleksandra Grzelik, and Gökhan Mutlu. Pangraphs as models of higher-order interactions. *arXiv preprint arXiv:2502.10141*, 2025.
 - [33] Dror Y. Kenett, Xuqing Huang, Irena Vodenska, Shlomo Havlin, and H. Eugene Stanley. Partial correlation analysis: applications for financial markets. *Quantitative Finance*, 15(4):569–578, April 2015.
 - [34] Juan Zhao, Yiwei Zhou, Xiujuan Zhang, and Luonan Chen. Part mutual information for quantifying direct associations in networks. *Proceedings of the National Academy of Sciences*, 113(18):5130–5135, May 2016.
 - [35] Elena Kuzmin, Benjamin VanderSluis, Wen Wang, Guihong Tan, Raamesh Deshpande, Yiqun Chen, Matej Usaj, Attila Balint, Mojca Mattiazzi Usaj, Jolanda van

- Leeuwen, Elizabeth N. Koch, Carles Pons, Andrius J. Dagilis, Michael Pryszlak, Jason Zi Yang Wang, Julia Hanchard, Margot Riggi, Kaicong Xu, Hamed Heydari, Bryan-Joseph San Luis, Ermira Shuteriqi, Hongwei Zhu, Nydia Van Dyk, Sara Sharifpoor, Michael Costanzo, Robbie Loewith, Amy Caudy, Daniel Bolnick, Grant W. Brown, Brenda J. Andrews, Charles Boone, and Chad L. Myers. Systematic analysis of complex genetic interactions. *Science*, 360(6386):eaao1729, April 2018.
- [36] Leonie Neuhäuser, Renaud Lambiotte, and Michael T Schaub. Consensus dynamics and opinion formation on hypergraphs. In *Higher-Order Systems*, pages 347–376. Springer, 2022.
- [37] Leonie Neuhäuser, Andrew Mellor, and Renaud Lambiotte. Multibody interactions and nonlinear consensus dynamics on networked systems. *Physical Review E*, 101(3):032310, 2020.
- [38] Iacopo Iacopini, Giovanni Petri, Alain Barrat, and Vito Latora. Simplicial models of social contagion. *Nature communications*, 10(1):2485, 2019.
- [39] Guilherme Ferraz de Arruda, Giovanni Petri, and Yamir Moreno. Social contagion models on hypergraphs. *Physical Review Research*, 2(2):023032, 2020.
- [40] Petar Veličković, Guillem Cucurull, Arantxa Casanova, Adriana Romero, Pietro Lio, and Yoshua Bengio. Graph attention networks. *arXiv preprint arXiv:1710.10903*, 2017.
- [41] Lyudmyla F Kozachenko and Nikolai N Leonenko. Sample estimate of the entropy of a random vector. *Problemy Peredachi Informatsii*, 23(2):9–16, 1987.
- [42] Alexander Kraskov, Harald Stögbauer, and Peter Grassberger. Estimating mutual information. *Physical review E*, 69(6):066138, 2004.
- [43] Brian C Ross. Mutual information between discrete and continuous data sets. *PloS one*, 9(2):e87357, 2014.
- [44] J Kurths and H Herzel. An attractor in a solar time series. *Physica D: Nonlinear Phenomena*, 25(1-3):165–172, 1987.
- [45] James Theiler, Stephen Eubank, André Longtin, Bryan Galdrikian, and J Doyné Farmer. Testing for nonlinearity in time series: the method of surrogate data. *Physica D: Nonlinear Phenomena*, 58(1-4):77–94, 1992.
- [46] Huili Wang, Sheng-Yan Lin, Fei-Fei Hu, An-Yuan Guo, and Hui Hu. The expression and regulation of hox genes and membrane proteins among different cytogenetic groups of acute myeloid leukemia. *Molecular genetics & genomic medicine*, 8:e1365, Sep 2020.
- [47] R. A. Alharbi, R. Pettengell, H. S. Pandha, and R. Morgan. The role of hox genes in normal hematopoiesis and acute leukemia. *Leukemia*, 27(5):1000–1008, 2013.
- [48] Huidong Guo, Yajing Chu, Le Wang, Xing Chen, Yang-peng Chen, Hui Cheng, Lei Zhang, Yuan Zhou, Feng-chun Yang, Tao Cheng, Mingjiang Xu, Xiaobing Zhang, Jianfeng Zhou, and Weiping Yuan. Pbx3 is essential for leukemia stem cell maintenance in mll-rearranged leukemia. *Int. J. Cancer*, 141(2):324–335, July 2017.
- [49] Ping Xiang, Xining Yang, Leo Escano, Ishpreet Dhillon, Edith Schneider, Jack Clemans-Gibbon, Wei Wei, Jasper Wong, Simon Xufeng Wang, Derek Tam, Yu Deng, Eric Yung, Gregg B. Morin, Pamela A. Hoodless, Martin Hirst, Aly Karsan, Florian Kuchenbauer, R. Keith Humphries, and Arefeh Rouhi. Elucidating the importance and regulation of key enhancers for human meis1 expression. *Leukemia*, 36(8):1980–1989, 2022.
- [50] Marouen Ben Guebila, Camila M Lopes-Ramos, Deborah Weighill, Abhijeet Rajendra Sonawane, Rebekka Burkholz, Behrouz Shamsaei, John Platig, Kimberly Glass, Marieke L Kuijjer, and John Quackenbush. "grand gene regulatory network database", 2023.
- [51] Marouen Ben Guebila, Camila M. Lopes-Ramos, Deborah Weighill, Abhijeet Rajendra Sonawane, Rebekka Burkholz, Behrouz Shamsaei, John Platig, Kimberly Glass, Marieke L. Kuijjer, and John Quackenbush. Grand: a database of gene regulatory network models across human conditions. *Nucleic Acids Res*, 50(D1):D610–D621, January 2022.
- [52] Amin Alishahi, Naoko Koyano-Nakagawa, and Yasushi Nakagawa. Regional expression of mtg genes in the developing mouse central nervous system. *Developmental Dynamics*, 238(8):2095–2102, 2009.